

The first migration method that is equally effective for all acquired frequencies for imaging and inverting at the target and reservoir

Arthur B. Weglein*, Yanglei Zou*, Qiang Fu*, Fang Liu*, Jing Wu*, Chao Ma*, Robert H. Stolt†, Xinglu Lin*, and James D. Mayhan*

Summary

There is an industry wide interest in acquiring lower frequency seismic data. There is also an interest in assuring that the broadband data provides added value in processing and interpretation, to better resolve structure and to provide improved amplitude analysis at the target and at the reservoir. There are industry reports that when comparing the new and more expensively acquired broadband lower frequency data with conventional recorded data, taken over a same region, that these two datasets have the expected difference in frequency spectrum and appearance, but they provide little or no difference in structural improvement or added benefit for amplitude analysis at the target and reservoir. The methods that take recorded data and determine structure and perform amplitude analysis are migration and migration-inversion, respectively. There are two objectives of this paper: (1) to demonstrate that all current migration and migration inversion methods make high frequency asymptotic assumptions, that consequently do not provide for equal effectiveness at all recorded frequencies, at the target and reservoir. The consequence is that in the process of migration, they lose or discount the information in the newly acquired lowest frequency components in the broad band data, and (2) we address that problem, with the first migration method that will be equally effective at all frequencies at the target and reservoir, and will allow the broad band lower frequency data to provide improved structure and more effective amplitude analysis.

Seismic acquisition and seismic processing must be consistent and aligned to provide interpretive value from broad band data.

Introduction

Migration methods that use wave theory for seismic imaging have two components: (1) a wave propagation model, and (2) an imaging condition.

We will examine each of these two components in this paper. After a brief general introduction, the focus will be on the specific topic of this paper: the frequency fidelity of migration algorithms.

That analysis leads to a new and first migration that is equally effective at the target and/or the reservoir. A paper, Weglein (2016), provides a detailed development of

this new migration method. In that paper, the new migration method is used to provide a definitive response to the role of primaries and multiples in seismic processing. This paper focuses on the frequency fidelity properties of all current and the new migration method.

For the imaging principle component, a good reference to start with is Jon Claerbout's 1971 landmark contribution. He listed three imaging principles: the exploding-reflector model which is for stacked or zero offset data. We call this Claerbout imaging principle I. The second imaging principle is the time space coincidence of up and downgoing waves. Waves propagate down from the source, are incident on the reflector and the reflector then generates a reflected up-going wave. According to Claerbout II (CII), the reflector exists at the location in space where the wave that is downward propagating from the source and the up wave from the reflector are at the same time and space.

Claerbout III (CIII) imaging starts with surface source and receiver data, and predicts what a source and receiver would record inside the earth. The CIII imaging principle then arranges the predicted source and receiver to be coincident and asks for $t = 0$. If the predicted coincident source and receiver experiment at depth is proximal to a reflector you get a non-zero result at time equals zero. CIII provides a direct and definitive yes or no at every subsurface point.

These three imaging conditions will give exactly the same result for a normal incident spike plane wave on a single horizontal reflector.

Claerbout II and III are of central industry interest today, since we currently process pre-stacked data. Imaging condition II and III will produce different results for a separated source and receiver located in a homogeneous half space above a single horizontal reflector. That difference forms a central and key message of this paper.

Before we undertake that comparison, let us take a look at a realization of the CIII imaging principle. Stolt's 1978 landmark contribution realized CIII imaging in the Fourier domain.

Stolt FK migration is

$$\begin{aligned} M^{stolt}(x, z) &= \frac{1}{(2\pi)^3} \iiint d\omega dx_g dx_s dk_{sx} \\ &\times \exp(-i(k_{sz}z + k_{sx}(x - x_s))) \\ &\times \int dk_{gx} \exp(-i(k_{gz}z + k_{gx}(x - x_s))) \\ &\times \int dt \exp(i\omega t) D(x_g, x_s, t). \end{aligned} \quad (1)$$

*M-OSRP, 617 Science & Research Bldg. 1, University of Houston, Houston, Texas 77204.

†2622 Mockingbird Drive, Ponca City, Oklahoma 74604.

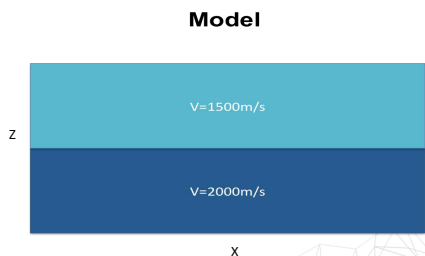


Fig. 1: A numerical example of Claerbout II imaging (current leading edge RTM) for a single reflector with a homogeneous velocity model (one shot gather) (Yanglei Zou and Weglein, 2014).

The weighted sum of recorded data, summed over receivers basically predicts the receiver experiment at depth, for a source on the surface. The sum over sources predicts the source in the subsurface, as well. Then the predicted source and receiver experiment is output for a coincident source and receiver, and at time equals zero; it defines a CIII image. Each step (integral) in this Stolt Fourier form of CIII has a specific physically interpretable purpose towards the CIII image.

Stolt made two extensions to Claerbout III. One was retaining the k_h information, angle dependent information at the target for structure and amplitude analysis, and in addition, introduced a point reflectivity. That point reflectivity automatically provides the specular reflection coefficient if there is one. It also provides a point reflectivity, an operator, which you can use for structure, which is non-planar, and to perform subsequent amplitude analysis. Those two extensions to get plane wave reflection coefficients and point reflectivity are only realizable in Claerbout III. Claerbout II cannot be extended and generalized in these two ways. Claerbout II is the basis and starting point for all current RTM methods. Hence, all RTM methods have certain intrinsic limitations, in terms of the ability to interpret images.

Claerbout II imaging

$$I(\vec{x}) = \sum_{\vec{x}_s} \sum_{\omega} S'(\vec{x}_s, \vec{x}, \omega) R(\vec{x}_s, \vec{x}, \omega). \quad (2)$$

R is the reflection data (for a shot record), run backwards, and S is the source wavefield.

The CII imaging is somewhat ad-hoc and not nearly on the same firm physical foundation and as interpretable as CIII.

We compare the CII and CIII where it is not a propagation issue, and where the structure is simple, that is, we consider a homogeneous medium above a single horizontal reflector. We will apply Claerbout II and Claerbout III and examine the differences.

In Figure 1, we see the model. The migration velocity here is 1500m/s.

Figure 2 is the result from Claerbout II for one shot record. There is an inconsistency in the image. The bot-

Migration method effective for all frequencies

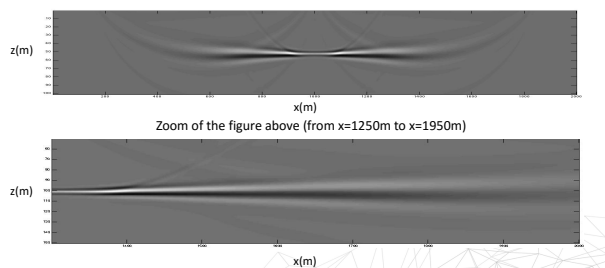


Fig. 2: A numerical example of Claerbout II imaging (current leading edge RTM) for a single reflector with a homogeneous velocity model (one shot gather) (Yanglei Zou and Weglein, 2014).

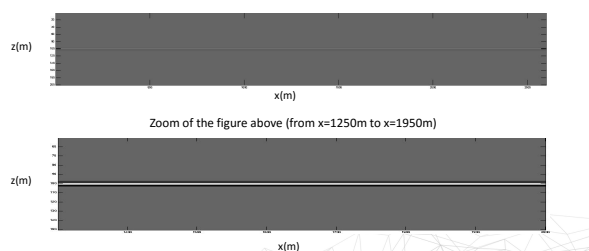


Fig. 3: A numerical example of Claerbout III Stolt migration for a single reflector (Yanglei Zou and Weglein, 2014).

tom image in Figure 2 shows a blow up to see the lateral inconsistency in the CII image. If you want to associate the image with something like structure and/or reflectivity, you are not obtaining something that is consistent in the simplest possible example.

Figure 3 shows the equivalent one shot record image of the Claerbout III Stolt migration.

Stolt's CIII produces a consistent and interpretable image. What people do in practice, with CII for one shot record is they stack over sources. They treat the CII algorithm as if it was intrinsically flawed and noisy. In Claerbout III, the sum over receivers, dx_g , is required to bring the receiver down, the sum over sources, dx_s , is required to bring the source down.

The sum over sources in Claerbout III is not fixing something that is inconsistent and intrinsically amiss, as the sum over sources seeks to mitigate in Claerbout II. There is no physics in CII to the sum over sources.

Now set the migration velocity be a discontinuous function c_0 over c_1 in Figure 4. In Figure 5, we perform Claerbout II for one trace, one source and one receiver and output the result. You find this ellipse and these (in)famous rabbit ears due to the c_0 , c_1 migration velocity model. Faqi Liu, et al, have provided a method to remove rabbit ears in Claerbout II when imaging with a discontinuous velocity.

Even for the single horizontal reflector and with rabbit ear removal the CII image is not consistent. And in fact,

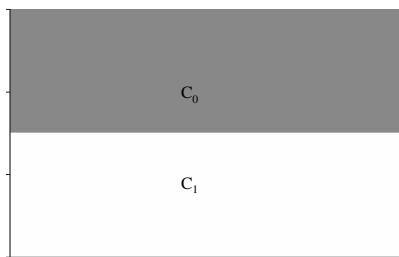


Fig. 4: The velocity model.

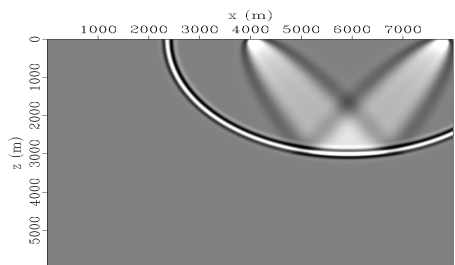


Fig. 5: Claerbout II RTM image for one trace.

the reduction or removal of the rabbit ears can have a negative impact on the image itself. Let's compare this to Claerbout III.

The new CIII migration in Figure 6 for two way propagating waves (from equation 4) produces the coincident source and receiver above and below the reflector with a light and dark amplitude for R_1 and $-R_1$, respectively. There are no rabbit ears in the new CIII (equation 4). With this new two way wave propagating CIII migration, you can, e.g., obtain the reflection coefficient from above and from below a top salt reflector.

How do high frequency approximations/assumptions enter a migration algorithm?

How do you know if a migration method has made a high

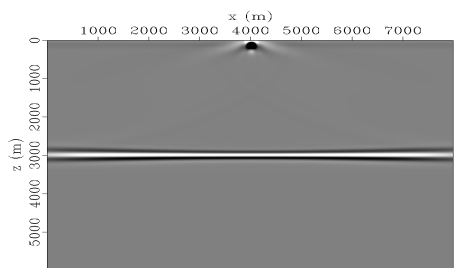


Fig. 6: Claerbout II RTM image after artifacts removal. Please note the inconsistent image along the reflector.

Migration method effective for all frequencies

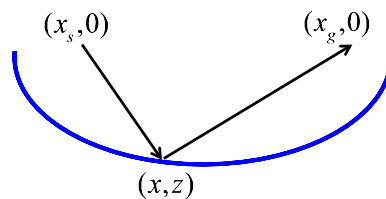


Fig. 7: (1) If there is a travel time curve of candidate images within the method, it is a high frequency "ray theory" approximation/assumption. $t = r/c$ where, $r = r_g + r_s = \sqrt{(x_g - x)^2 + z^2} + \sqrt{(x_s - x)^2 + z^2}$.

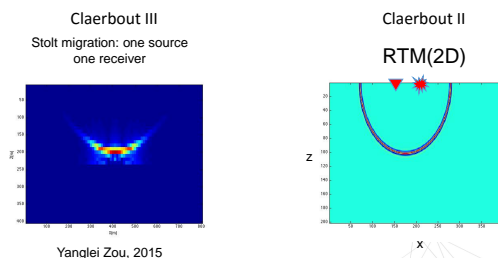


Fig. 8: Imaging Conditions and High Frequency Assumptions. Left panel: No high frequency assumption. Right panel: High frequency assumption.

frequency approximation?

If you have a picture shown in Figure 7 (a set of candidate images in the migration process) at any step or stage in the migration method, then the migration method has made an asymptotic high frequency assumption/approximation. As we saw for Claerbout II, for one source and one receiver, the image is an ellipse. If you have a travel time ellipse of candidate images, that's an absolute and definite indication that the migration method has made a high-frequency approximation. This picture (Figure 7) is a ray-theory picture.

In Figure 8, we compare the results of CII and CIII for one source and one receiver, CII provides an ellipse while CIII does not. CIII provides a local image. In CII, in this simplest case, where the data is perfect and the medium is homogeneous, the contribution from one source and one receiver, you obtain a set of candidates. CIII will never provide candidates. CIII will bring you to a point in the earth where you have a coincident source and receiver experiment. At time equals zero, if there is a non zero result, you are at a reflector, there is a structure there, not a possible or candidate structure. The result from Claerbout II is a set of candidates of possible structure. That's intrinsic to Claerbout II, hence intrinsic to all current RTM. So, if you are doing RTM today and any extension of it, understand that you have made a high frequency approximation in your migration methods. Similarly Kirchhoff migration is an asymptotic high frequency approximate of Stolt CIII (see Figure 9)

There are other ways that high frequency approximations can enter migration methods. If you made a stationary phase approximation, the migration method is a high fre-

Kirchhoff migration (2D)

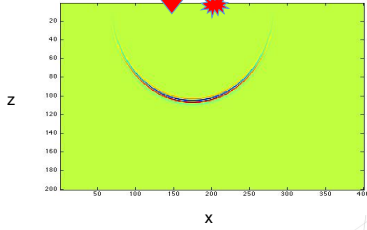


Fig. 9: Kirchhoff migration for a single source and receiver (Yanglei Zou et al, 2015). High Frequency approximation from a stationary phase approximation.

quency approximation.

There is another more subtle way that high frequency approximations can enter migration methods. Let's say, we are in Claerbout III (we are predicting the source and receiver experiment at depth) and let's assume a smooth velocity model. If in that smooth velocity model, you were assuming at every point, that the wave is moving in one direction, then you have made a high frequency approximation, even though you are using Claerbout III imaging. The only time that the wave is moving in one direction at a given point is in a homogeneous medium. As soon as you have any deviation from homogeneous, at every point in that medium, part of that wave is moving down and part of wave is moving up. If you are assuming it is only moving in one direction at one point (e.g., using WKBJ or diving waves), you have made a high frequency approximation.

All CII imaging, i.e., all RTM methods today are from the imaging principle itself, high frequency approximations/assumptions regardless of how they are implemented. Equation 3 represents a Green's theorem formulation of CIII for one way waves and is equivalent to Stolt migration equation 1. G_0^{-D} is an anticausal Green's function that vanishes on the measurement surface. For a heterogeneous medium assuming one way propagation, at a point (even if you assume its overall downgoing and then upgoing, e.g., between source and reflector, and then separately, first downgoing and then upgoing from reflector to receiver) is a high frequency approximation, even if you are adopting a CIII imaging principle.

$$P = \int_{S_s} \frac{\partial G_0^{-D}}{\partial z_s} \int_{S_g} \frac{\partial G_0^{-D}}{\partial z_g} P dS_g dS_s \quad (3)$$

Prestack Stolt migration (Green, 1-way waves)

Equation 4 is the new migration method of this paper. It is a CIII imaging for a heterogeneous medium, that doesn't assume one-way propagation at either a point or separately, overall between source and reflector, and, reflector to receiver. G_0^{DN} is the Green's function for the heterogeneous medium that vanishes along with its normal derivative at the lower surface of the migration volume (Weglein et al., 2011b).



Fig. 10: The new M-OSRP Claerbout III (Stolt extended) migration for 2 way wave propagation. The example with c_0/c_1 velocity. The image both above and beneath the reflector. No "rabbit ears". Consistent image along the reflector. Light color image from above. Dark color image from below. (Qiang Fu and Weglein, 2015)

Equation 4 is the first migration method that is equally effective at all frequencies at the target and at the reservoir. Equation 4 was used in obtaining the result above and below the reflector in Figure 10.

$$P = \int_{S_s} \left[\frac{\partial G_0^{DN}}{\partial z_s} \int_{S_g} \left\{ \frac{\partial G_0^{DN}}{\partial z_g} P + \frac{\partial P}{\partial z_g} G_0^{DN} \right\} dS_g \right. \\ \left. + G_0^{DN} \frac{\partial}{\partial z_s} \int_{S_g} \left\{ \frac{\partial G_0^{DN}}{\partial z_g} P + \frac{\partial P}{\partial z_g} G_0^{DN} \right\} dS_g \right] dS_s \quad (4)$$

(Green, 2-way waves) for details see Weglein et al. (2011a,b) and F. Liu and Weglein (2014)

Conclusion

To obtain broad band benefit and added value requires effective deghosting and a migration method that treats all frequencies with equal effectiveness at the target and reservoir. This paper provides a first migration algorithm with those qualities and benefits. Seismic acquisition and processing must be consistent and aligned to provide interpretive value at the target and reservoir from broad-band data.

References

- Berkhout, A. J., 1980, Seismic migration, imaging of acoustic energy by wave field extrapolation, 1st ed.: Elsevier, Amsterdam/North Holland.
- Claerbout, J. F., 1971, Toward a unified theory of reflector mapping: *Geophysics*, **36**, 467–481.
- Fu, Q., A. B. Weglein, and F. Liu, 2015, (Short Note) Claerbout imaging condition III in 1.5D medium for two-way propagating wave by using the special Green's function doubly vanishing at the lower boundary: M-OSRP 2014-2015 Annual Report, 85–96.
- Gazdag, J., 1978, Wave equation migration with the phase-shift method: *Geophysics*, **43**, 1342–1351.
- Liu, F., and A. B. Weglein, 2014, The first wave equation migration RTM with data consisting of primaries and internal multiples: theory and 1D examples: *Journal of Seismic Exploration*, **23**, 357–366.
- Liu, F., G. Zhang, S. A. Morton, and J. P. Leveille, 2011, An effective imaging condition for reverse-time migration using wavefield decomposition: *Geophysics*, **76**, S29–S39.
- Mayhan, J. D., 2013, Wave theoretic preprocessing to allow the Inverse Scattering Series methods for multiple removal and depth imaging to realize their potential and impact: Methods, examples, and added value: PhD thesis, University of Houston.
- Mayhan, J. D., P. Terenghi, A. B. Weglein, and N. Chemingui, 2011, Green's theorem derived methods for preprocessing seismic data when the pressure P and its normal derivative are measured: 81st Annual International Meeting, SEG, Expanded Abstracts, 2722–2726.
- Mayhan, J. D., and A. B. Weglein, 2013, First application of Green's theorem-derived source and receiver deghosting on deep-water Gulf of Mexico synthetic (SEAM) and field data: *Geophysics*, **78**, WA77–WA89.
- Mayhan, J. D., A. B. Weglein, and P. Terenghi, 2012, First application of Green's theorem derived source and receiver deghosting on deep water Gulf of Mexico synthetic (SEAM) and field data: 82nd Annual International Meeting, SEG, Expanded Abstracts, 1–5.
- McMechan, G. A., 1983, Migration by extrapolation of time dependent boundary values: *Geophysical Prospecting*, **31**, 413–420.
- Robinson, E. A., 1986, Migration and the Mercator projection: *The Leading Edge*, **5**, 19–23.
- , 1998, Further to Norman Neidell's series. . . Holistic migration: *The Leading Edge*, **17**, 313–320.
- Robinson, E. A., and S. Treitel, 2000, Migration of seismic data, *in* *Geophysical Signal Analysis*: SEG, 15, 374–398.
- , 2008, Digital imaging and deconvolution: The ABCs of seismic exploration and processing: Society of Exploration Geophysicists.
- Ronen, S., and C. L. Liner, 2000, Least-squares DMO and migration: *Geophysics*, **65**, 1364–1371.
- Schleicher, J., M. Tygel, and P. Hubral, 1993, 3-D true-amplitude finite-offset migration: *Geophysics*, **58**, 1112–1126.
- Schneider, W. A., 1978, Integral formulation for migration in two and three dimensions: *Geophysics*, **43**, 49–76.
- Schultz, P. S., and J. W. C. Sherwood, 1980, Depth migration before stack: *Geophysics*, **45**, 376–393.
- Stolt, R. H., 1978, Migration by Fourier transform: *Geophysics*, **43**, 23–48.
- Stolt, R. H., and A. K. Benson, 1986, Seismic migration: theory and practice: Geophysical Press.
- Stolt, R. H., and A. B. Weglein, 1985, Migration and inversion of seismic data: *Geophysics*, **50**, 2458–2472.
- , 2012, Seismic imaging and inversion: Application of linear inverse theory: Cambridge University Press.
- Tang, L., J. D. Mayhan, J. Yang, and A. B. Weglein, 2013, Using Green's theorem to satisfy data requirements of multiple removal methods: The impact of acquisition design: 83rd Annual International Meeting, SEG, Expanded Abstracts, 4392–4396.
- Weglein, A. B., 2016, Multiples: signal or noise?: *Geophysics*. (Accepted 3.14.16 for publication).
- Weglein, A. B., S. A. Shaw, K. H. Matson, J. L. Sheiman, R. H. Stolt, T. H. Tan, A. Osen, G. P. Correa, K. A. Innanen, Z. Guo, and J. Zhang, 2002, New approaches to deghosting towed-streamer and ocean-bottom pressure measurements: 72nd Annual International Meeting, SEG, Expanded Abstracts, 2114–2117.
- Weglein, A. B., and R. H. Stolt, 1999, Migration-inversion revisited (1999): *The Leading Edge*, **18**, 950–952, 975.
- Weglein, A. B., R. H. Stolt, and J. D. Mayhan, 2011a, Reverse-time migration and Green's theorem: Part I — The evolution of concepts, and setting the stage for the new RTM method: *Journal of Seismic Exploration*, **20**, 73–90.
- , 2011b, Reverse time migration and Green's theorem: Part II — A new and consistent theory that progresses and corrects current RTM concepts and methods: *Journal of Seismic Exploration*, **20**, 135–159.
- Whitmore, N. D., 1983, Iterative depth imaging by back time propagation: 53rd Annual International Meeting, SEG, Expanded Abstracts, 382–385.
- Wu, J., and A. B. Weglein, 2014, Elastic Green's theorem preprocessing for on-shore internal multiple attenuation: Theory and initial synthetic data tests: 84th Annual International Meeting, SEG, Expanded Abstracts, 4299–4304.
- , 2015a, Preprocessing in displacement space for on-shore seismic processing: removing ground roll and ghosts without damaging the reflection data: 85th Annual International Meeting, SEG, Expanded Abstracts, 4626–4630.
- , 2015b, Preprocessing in the PS space for on-shore seismic processing: removing ground roll and ghosts without damaging the reflection data: 85th Annual International Meeting, SEG, Expanded Abstracts, 4740–4744.
- Yang, J., J. D. Mayhan, L. Tang, and A. B. Weglein, 2013, Accommodating the source (and receiver) array in free-surface multiple elimination algorithm: Impact on interfering or proximal primaries and multiples: 83rd Annual International Meeting, SEG, Expanded Abstracts,

- 4184–4189.
- Zhang, J., 2007, Wave theory based data preparation for inverse scattering multiple removal, depth imaging and parameter estimation: analysis and numerical tests of Green's theorem deghosting theory: PhD thesis, University of Houston.
- Zhang, J., and A. B. Weglein, 2005, Extinction theorem deghosting method using towed streamer pressure data: analysis of the receiver array effect on deghosting and subsequent free surface multiple removal: 75th Annual International Meeting, SEG, Expanded Abstracts, 2095–2098.
- , 2006, Application of extinction theorem deghosting method on ocean bottom data: 76th Annual International Meeting, SEG, Expanded Abstracts, 2674–2678.
- Zhang, Y., S. Xu, N. Bleistein, and G. Zhang, 2007, True-amplitude, angle-domain, common-image gathers from one-way wave-equation migrations: *Geophysics*, **72**, S49–S58.
- Zhang, Y., and G. Zhang, 2009, One-step extrapolation method for reverse time migration: *Geophysics*, **74**, A29–A33.
- Zhou, H., and G. A. McMechan, 1999, Parallel Butterworth and Chebyshev dip filters with applications to 3-D seismic migration: *Geophysics*, **64**, 1573–1578.
- Zou, Y., and A. B. Weglein, 2015, An internal-multiple elimination algorithm for all first-order internal multiples for a 1D earth: 85th Annual International Meeting, SEG, Expanded Abstracts, 4408–4412.